Available online at www.sciencedirect.com
ScienceDirect
International Journal of Pharmaceutics 322 (2006) 36–43
INTERNATIONAL JOURNAL OF PHARMACEUTICS
www.elsevier.com/locate/ijpharm

Swellable drug–polyelectrolyte matrices (SDPM) of alginic acid Characterization and delivery properties

María V. Ramírez Rigo, Daniel A. Allemandi, Ruben H. Manzo *

Departamento de Farmacia, Facultad de Ciencias Químicas, Universidad Nacional de Córdoba, Ciudad Universitaria, 5000 Córdoba, Argentina

Received 23 September 2005; received in revised form 22 February 2006; accepted 11 May 2006
Available online 17 May 2006

Abstract

This study deals with the development and characterization of the delivery properties of swellable drug–polyelectrolyte matrices (SDPM) of alginic acid (AA). Complexes $(AA–D)_x$ in solid state were obtained by neutralization of AA with different molar proportions (x) of model basic drugs (D), in which D is atenolol, metoclopramide and propranolol. They were characterized by DSC, IR and X-ray diffraction.

Matrices prepared by compaction of $(AA–D)_x$ alone or in a mixture with sodium alginate (NaAA) were subjected to measurements of solvent up-take, release kinetics and erosion in three media (water, buffer of pH 6.8 and 0.01 M HCl). In addition, the dynamics of swelling was also evaluated. All SDPM assayed exhibited a remarkable zero order of delivery in water and buffer of pH 6.8 and also in two-step delivery experiments: 2 h in acid medium followed by a second step at pH 6.8. Experimental results indicate that the erosion of the hydrogel layer is the main delivery process. Delivery rate, can be modulated either by varying the composition of $(AA–D)_x$ or by diluting it with NaAA.

Keywords: Erodible matrices; Polyelectrolyte–drug matrices; Drug delivery; Controlled release; Alginic acid

1. Introduction

This paper deals with the characterization and delivery properties of swellable drug–polyelectrolyte matrices (SDPM), which are obtained by compaction of powdered complexes of a polyelectrolyte (PE) fully or partially neutralized with an ionizable drug (D). Therefore, SDPM contain a molecular dispersion of D in the mass of the matrix since D is ionically bonded to the functional groups of PE.

We have previously evaluated SDPM obtained with carbomer (C) as acid polyelectrolyte (Jimenez-Kairuz et al., 2005), which exhibited interesting delivery properties and can find a place as a new class of swellable hydrophilic matrices in the design of delivery systems.

Here, we report the characterization of delivery properties of SDPM prepared with $(AA–D)_x$ complexes of alginic acid (AA) neutralized with different molar proportions (x) of model basic drugs. With such purpose three D having different aqueous solubilities (atenolol (At), 12.80 mg/ml; metoclopramide (Me), 0.20 mg/ml propranolol (Pr), 0.13 mg/ml; (Pitré and Stradi, 1987; Jimenez-Kairuz, 2004)) were selected to prepare $(AA–D)_x$ complexes in solid state. Besides, mixed matrices of $(AA–D)_x$ with sodium alginate (NaAA) were also examined.

Both AA and NaAA are excipients widely used in solid oral dosage forms, currently regarded as binders or desintegrants (Wade and Weller, 1994). It is also known that NaAA retards drug release (Klaudianos, 1978). It has been also used in drug microencapsulation (Bodmeier and Wang, 1993) and in the design of matrices, alone or in combination with calcium salts (chloride, acetate and gluconate) to generate in situ a strong gel of calcium alginate (Østberg et al., 1994; Rubio and Ghaly, 1994; Giunchedi et al., 2000; Holte et al., 2003).

Although there are a number of valuable contributions in this field, a detailed description of the role of the interaction between carboxylic groups of AA and basic groups of D in drug delivery is not available. This report would also contribute with more detailed information on this point.

On the other hand, the results presented here will be compared with those previously obtained with C as PE.

Therefore, with the aim of getting information about delivery properties of $(AA–D)_x$ complexes, matrices of $(AA–D)_x$ alone

* Corresponding author. Tel.: +54 351 4334163; fax: +54 351 4334127.
E-mail address: rubmanzo@mail.fcq.unc.edu.ar (R.H. Manzo).

0378-5173/$ – see front matter © 2006 Elsevier B.V. All rights reserved.
doi:10.1016/j.ijpharm.2006.05.025

or in a mixture with NaAA were subjected to measurements of solvent up-take, release kinetics and erosion in three media. In addition, the dynamics of swelling was also evaluated.

2. Materials and methods

2.1. Materials

The following materials were used: AA from *Macrocystis pyrifera* (PA grade, Sigma Chemical, St. Louis, USA), NaAA (USP-Pharmacopoeia grade, Montreal, Córdoba, Argentina), atenolol, metoclopramide hydrochloride, propranolol hydrochloride (Pharmaceutical grade, Parafarm, Bs. As., Argentina), ethanol (USP-Pharmacopoeia grade, Porta, Córdoba, Argentina). Free bases of Me and Pr were obtained by neutralization of their hydrochloride solutions with NaOH. Solid products obtained were filtered, washed with distilled water and dried in oven at 50 °C to constant weight. The equivalents of carboxylic groups per gram of AA (4.71×10^{-3}) were assayed by acid–base titration.

2.2. $(AA–D)_x$ complexes

Subscript x refers to the mol% of basic drug that neutralizes the carboxylic acid groups of AA. Complexes in solid state were prepared by mixing in a mortar AA with an appropriate amount of D to obtain $(AA–D)_{50}$ or $(AA–D)_{75}$ and adding water or ethanol to get a semisolid paste. Products were dried in oven at 50 °C to constant weight, powdered and sieved to select particle sizes in the range 75–212 μm.

Characterization of $(AA–D)_{50}$ complexes was performed by FT-infrared spectroscopy (FT-IR) (Avatar 360, ESP Nicolet, with KBr 1.5% disks), powder X-ray diffraction (Rigaku Miniflex diffractometer, scan range was 5–70°) and differential scanning calorimetry (DSC) (TA-Instruments Modulated-DSC 2920, Universal Analysis-NT software, 1–2 mg samples were run at 10 °C/min ramp in hermetic pans under nitrogen atmosphere, flowing at 60 ml/min) (Bonferoni et al., 2000; Jimenez-Kairuz et al., 2005). Physical mixtures of AA and D and AA or D alone were also assayed.

2.3. $(AA–At)_x$ dispersions

They were obtained by neutralizing a 5% aqueous dispersion of AA with the appropriate amount of At under stirring. Hydrogel viscosities were determined at 25 °C, 100 s^{-1}, in a Haake viscometer VT500 equipped with NV or MV1 sensors.

2.4. SDPM preparation

Matrices of $(AA–D)_x$ alone or mixed with different proportions of NaAA ($(AA–D)_x$ + NaAA) were obtained by compacting 200–400 mg of powder at 2 tonnes for 30 s in a hydraulic press equipped with flat punches 12.8 mm in diameter. Matrices hardness was in the range of 3–4 kg, determined in a Hardness tester DU4, AVIC.

2.5. Wetting and swelling

Wetting and swelling were evaluated by means of up-take profiles and the dynamics of radial front movements.

2.5.1. Solvent up-take

Sorption of water or aqueous solution (buffer of pH 6.8 and 0.01 M HCl) by SDPM was determined using a device described by Nogami et al. (1969) and Llabot et al. (2002).

2.5.2. Radial front movement

Erosion and swelling fronts were measured according to Jimenez-Kairuz et al. (2005) by a technique previously reported by several authors (Bettini et al., 1994; Colombo et al., 1995, 1996, 1999; Ferrero et al., 2000). The diffusion front was determined by adding to the delivery medium a small amount of an acid–base indicator, a previously reported technique (Jimenez-Kairuz et al., 2005). A mixture of bromocresol green sodium salt (0.05%) and methyl orange (0.01%) was selected as the acid–base indicator (orange at pH < 4.5 and green or blue at pH > 4.5) (The Merck Index, 1996).

2.6. Release from SDPM

Release of D was measured in a USPXXIV dissolution apparatus 1 (Hanson Res., USA) at 50 or 100 rpm and 37 °C using 900 ml of degassed dissolution medium (distilled water, USP-intestinal solution without enzyme, or 0.01 N HCl solution). The basket apparatus was selected to avoid sticking of the matrices on the wall of the dissolution vessel. Standard baskets of 40-mesh size were used.

Samples of 5 ml were taken at defined time intervals, filtered through a teflon membrane (10 μm pore size) and replaced with equivalent amounts of fresh medium preheated to 37 °C. D released was spectrophotometrically determined.

Release rates were regarded as the slopes of the straight lines obtained by applying minimum squares method to the experimental points.

The same experimental device and conditions were used to measure matrix erosion according to Sinha Roy and Rohera (2002). With such purpose, SDPM were removed from the medium at determined time intervals and lightly patted using tissue paper. Then, they were dried at 60 °C until constant weight to determine percent mass loss:

$$\text{Mass loss } (\%)_t = \frac{\text{original weight} - \text{remaining (dry) weight}_t}{\text{original weight}} \times 100.$$

2.7. Release from $(AA–At)_x$ dispersion

Release of At from $(AA–At)_{100}$ dispersion was measured in a bicompartimental device, limited by a dialysis cellulose membrane (12000d, Sigma) as described by Vilches et al. (2002). The sample compartment was loaded with 20 ml of the dispersion and kept in contact with 250 ml of receptor medium (distilled water or 0.9% NaCl solution) at 37 °C.

Samples of 5 ml were taken at defined time intervals and were replaced with equivalent amounts of fresh medium. Release of At was spectrophotometrically determined.

All the experiments were conducted in triplicate, mean values are reported.

3. Results and discussion

3.1. $(AA–D)_x$ complexes

A preliminary characterization of the solid state of these materials was obtained as follows: FT-IR spectra of $(AA–D)_x$ show a decrease of the strong band at 1740 cm^{-1} ascribed to the carbonyl of undissociated carboxylic groups of alginic acid ($(AA–Pr)_{50}$, 1754 cm^{-1}; $(AA–Me)_{50}$, 1731 cm^{-1}; $(AA–At)_{50}$, 1740 cm^{-1}) (Huang et al., 1999). Such changes are paralleled by the increase of the band ascribed to the antisymmetric stretching vibration of dissociated carboxylic groups of AA. In detail, $(AA–Pr)_{50}$, $(AA–Me)_{50}$ and $(AA–At)_{50}$ show a band at 1600, 1623 and 1613 cm^{-1}, respectively. The band ascribed to the symmetric stretching vibration of COO^- at ~1400 cm^{-1} could not be observed, probably because it overlaps with bands of D.

On the other hand, the absorption band associated with the protonated nitrogen (Conley, 1979) is observed at 2648 cm^{-1} in $(AA–Me)_{50}$ at 2700 cm^{-1} in $(AA–Pr)_{50}$ and at 2715 cm^{-1} in $(AA–At)_{50}$.

Besides, the information provided by the DSC profiles of the complexes is also in line with that obtained from IR spectra. Fig. 1 shows an example of typical comparative DSC profiles. They were obtained by running the complex $(AA–At)_{50}$ and a physical mixture of AA and At. As can be seen in the $(AA–At)_{50}$ run the melting endotherm corresponding to crystalline At (153 °C) is not present. Besides, this profile is quite similar to those of AA and NaAA reported by Soares et al. (2004), since both, the endotherm attributed to dehydration process of the polyelectrolyte (75 °C) and the exotherm associated with decomposition processes (at about 210 °C) are observed.

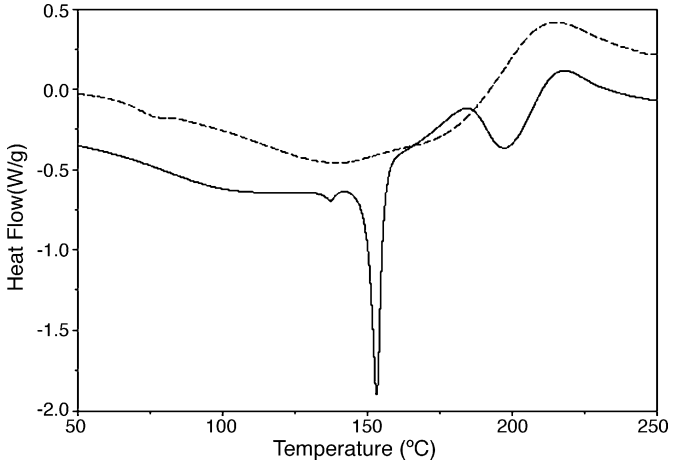

Fig. 1. DSC profiles of (- - -) $(AA–At)_{50}$ and (—) physical mixture of AA and At.

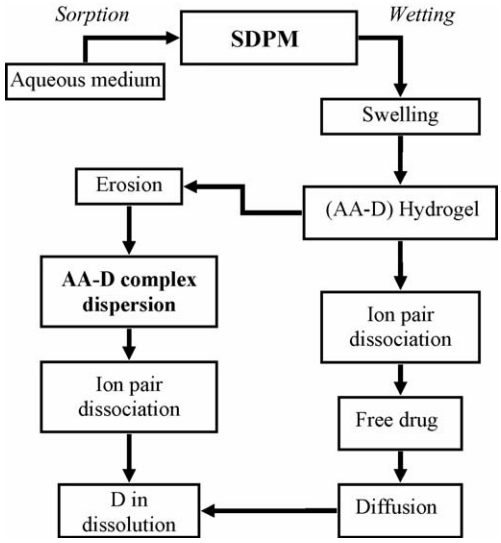

Scheme 1.

The same pattern was observed by X-ray powder diffraction were the crystalline structure of D could not be recognized in the complex.

All these results confirm the ionic interaction polyelectrolyte–drug in $(AA–D)_x$ complexes and are consistent with recently published results on the interaction between NaAA and methylene blue or 4-phenylazoaniline in microparticles (Tu et al., 2005).

3.2. SDPM

A matrix in contact with an aqueous medium originates the delivery process depicted in Scheme 1.

3.3. Wetting and swelling

3.3.1. Solvent up-take

Fluid sorption of SDPM prepared with $(AA–At)_{50}$ was measured in three media (water, buffer of pH 6.8 and 0.01 M HCl) displaying quite similar profiles. Sorption rate in water was slow and decreased with time, requiring about 60 min to take a mass of fluid equivalent to half of the initial matrix weight (Fig. 2). Incorporation of NaAA into the matrix favors the up-take process, keeping the initial rate of sorption almost constant along time as is shown in the figure.

3.3.2. Dynamics of swelling

Fig. 3 is a typical example of the front dynamics observed under experimental conditions. It can be seen there that the first stages of wetting and swelling produce a modest increase of the diameter of the matrix, which after that remains almost constant along time (erosion front). At the same time, the radius of the unwetted portion of the matrix (swelling front) decreases at almost a constant rate. Therefore, the hydrogel layer is progressively expanded. The shift of the acid–base indicator from orange to green-blue in going from inner to outer zones of the layer, which is regarded as the diffusion front in the figure, can

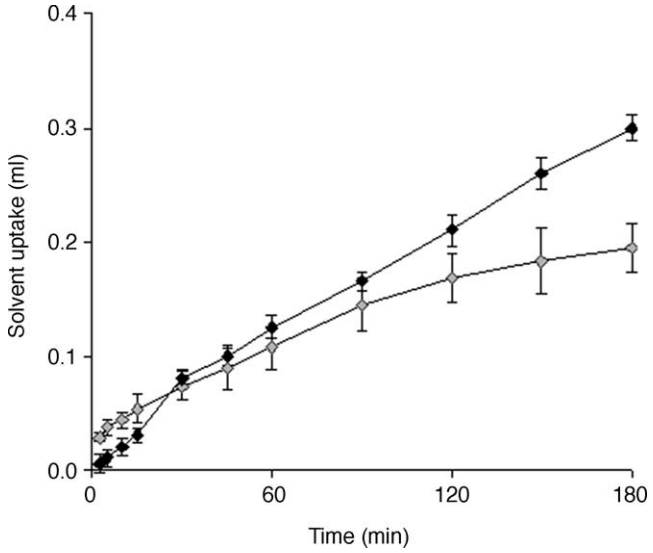

Fig. 2. Water up-take of matrices of 200 mg: (◇) $(AA–At)_{50}$, (◆) $(AA–At)_{50}$ + NaAA (1:2).

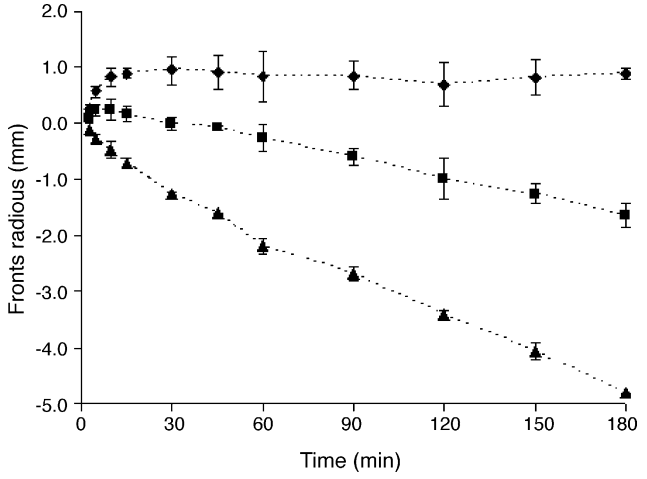

Fig. 3. Front movements of the $(AA–At)_{50}$ matrix in water: (◆) erosion front, (■) diffusion front, (▲) swelling front.

be associated with the rise of concentration of free drug [D]. As previously suggested (Jimenez-Kairuz et al., 2005), the rise of [D] would be a consequence of the degree of hydration and subsequent relaxation of the (AA–D) complex to produce some degree of dissociation of ionic pairs.

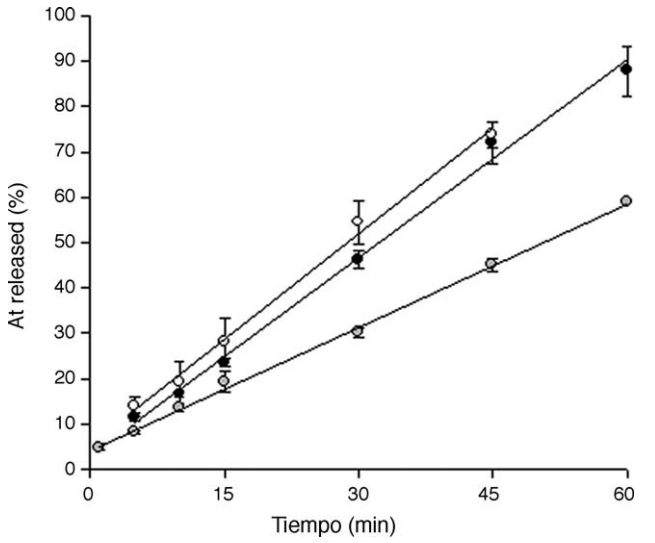

Fig. 4. Release kinetics of At from $(AA–At)_{50}$ matrices in: (●) distilled water, (◎) HCl 0.01N solution, (○) USP-intestinal solution without enzyme.

3.4. Release kinetics in water, buffer of pH 6.8 and 0.01 M HCl

Drug release from matrices of $(AA–At)_{50}$ and $(AA–At)_{75}$ in water exhibited a constant delivery rate (zero order kinetics) along the whole experiment, that was proportional to the amount of At in the matrix (Table 1a). The first composition was also assayed in buffer of pH 6.8 exhibiting both order and rate similar to that found in water (Fig. 4). However, as it is also shown in the figure, in acid medium the rate was slower and, as it is shown in Fig. 5, after 60% of delivery it drops departing from the initial zero order.

Since delivery rates appear to be relatively high for extended oral delivery systems and having observed that they are directly related to the proportion of At in the matrix, the effect of dilution of the complex was investigated. With such purpose NaAA was used to get mixed matrices of $(AA–At)_{50}$ (100 mg) with increasing proportions of NaAA (1:1, 1:2 and 1:3) as it is also reported in Tables 1a and 1b. These matrices in water as well as in pH 6.8 solution maintain the zero order delivery until D was completely released, but rates were slower as the proportion of NaAA was increased. In acid medium delivery rates follow the same trend but delivery profiles exhibit a break point after which rates became slower as it is shown in Fig. 5.

Table 1a
Matrix composition and drug release in water at 50 rpm

Matrices	Matrix weight (mg)	At in the matrix (mg)	At release distilled water		
			Slope (%/min)	Intercept	r^2 (n)[a]
$(AA–At)_{50}$	200	77	1.45	3.08	0.996 (6)
$(AA–At)_{75}$	200	115.5	2.05	−1.25	0.994 (6)
$(AA–At)_{50}$ + NaAA					
(a) (1:1)	200	38.5	1.14	−13.95	0.993 (6)
(b) (1:2)	300	38.5	0.82	−7.34	0.998 (7)
(c) (1:3)	400	38.5	0.56	−10.49	0.997 (6)

[a] n, number of points. They cover a range of 0–80% of delivery.

Table 1b
Drug release in USP-intestinal solution without enzyme and HCl 0.01N solution at 50 rpm

Matrices	At release								
	USP-intestinal solution			HCl 0.01N solution (first portion)			HCl 0.01N solution (second portion)		
	Slope (%/min)	Intercept	r^2 (n)[a,b]	Slope (%/min)	Intercept	r^2 (n)[a]	Slope (%/min)	Intercept	r^2 (n)[a]
$(AA–At)_{50}$	1.55	2.28	0.995 (5)	0.91	4.17	0.998 (7)[b]	–	–	–
$(AA–At)_{50}$ + NaAA									
(a) (1:1)	1.01	−7.87	0.993 (6)	0.46	0.64	0.994 (8)	0.10	51.37	0.985 (5)
(b) (1:2)	0.49	−1.73	0.997 (7)	0.32	3.63	0.990 (5)	0.11	31.27	0.994 (5)
(c) (1:3)	0.38	−1.31	0.998 (7)	0.20	−1.84	0.996 (7)	0.11	11.81	0.996 (5)

[a] n, number of points.
[b] Points cover a range of 0–80% of delivery.

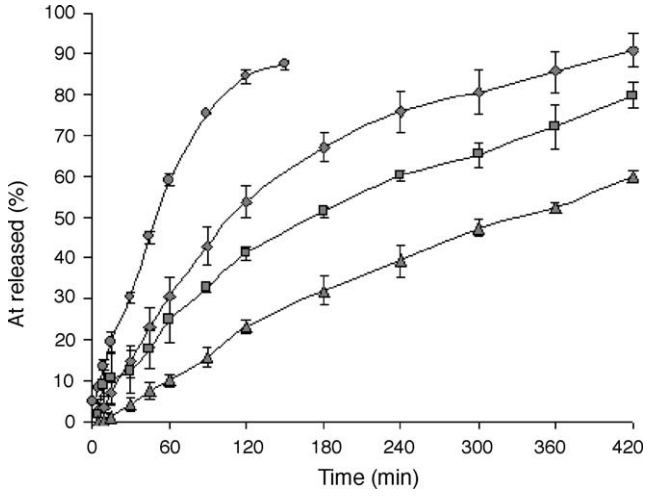

Fig. 5. At release profiles in HCl 0.01N solution from different matrices: (○) $(AA–At)_{50}$, $(AA–At)_{50}$ + NaAA—(◇) (1:1), (□) (1:2), (△) (1:3).

However, the mixed matrices subjected to two-step delivery experiments, consisting of 2 h in acid medium followed by a second step at pH 6.8, shown a remarkable constant delivery rate along the whole time tested as reported in Fig. 6.

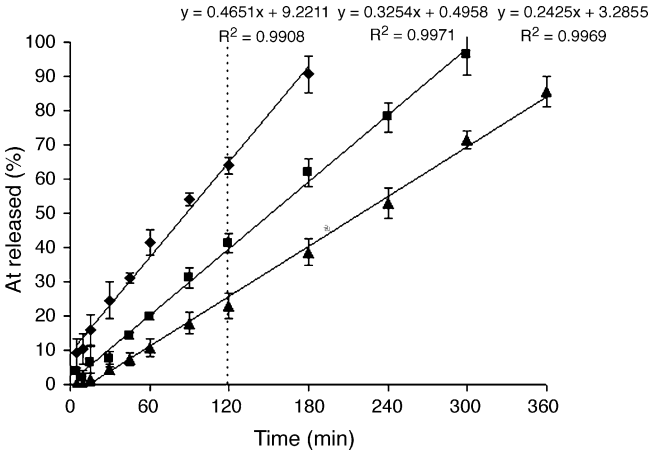

Fig. 6. Release profiles of At from mixed matrices ($(AA–At)_{50}$ + NaAA (♦) (1:1), (■) (1:2), (▲) (1:3)) in 0.01N HCl solution (0–120 min) and furtherly in USP-intestinal solution without enzyme (120–360 min).

3.5. The mechanism of delivery

Zero order kinetics in matrix delivery is currently associated with the prevalence of erosion mechanisms (Munday and Cox, 2000; Zuleger and Lippold, 2001; Ughini et al., 2004). Such point was addressed by means of a set of experiments in which the variation of the mass of the matrix along time was determined. A typical result is shown in Fig. 7, which shows the clear parallelism between At delivery and matrix erosion. Similar results were obtained with matrices of different compositions of $(AA–At)_{50}$ + NaAA.

In addition, a lowering of the stirring rate from 100 to 50 rpm was accompanied by a concomitant lowering of delivery rate (Table 2) as it is currently found in erodible systems (Zuleger and Lippold, 2001; Kavanagh and Corrigan, 2004).

Is clear now that the zero order of delivery observed under different conditions is a consequence of a balance between the expansion and erosion of the hydrogel layer that results in an almost constant surface area of the matrix in contact with the dissolution medium.

The mechanism of drug delivery from PE-D hydrogels was extensively discussed in previous papers (Jimenez-Kairuz et al., 2002, 2003; Jimenez-Kairuz, 2004; Vilches et al., 2002). On

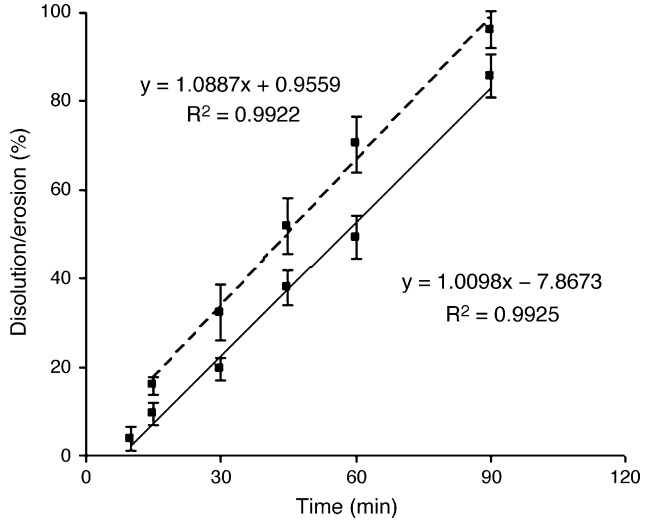

Fig. 7. Relationship between At release (—) and matrix erosion (- - -) of the matrix $(AA–At)_{50}$ + AANa (1:1) in USP-intestinal solution without enzyme.

Table 2
Comparison of At release at 100 and 50 rpm in USP-intestinal solution without enzyme

Matrix	At release					
	50 rpm			100 rpm		
	Slope (%/min)	Intercept	r^2 (n)[a]	Slope (%/min)	Intercept	r^2 (n)[a]
$(AA–At)_{50}$	1.55	2.28	0.995 (5)	3.04	6.50	0.990 (6)
$(AA–At)_{50}$ + NaAA (1:3)	0.38	−1.31	0.998 (7)	0.54	2.28	0.998 (11)

[a] n, number of points. They cover a range of 0–80% of delivery.

Table 3
Matrix composition and drug release in USP-intestinal solution at 50 rpm

Matrices	Matrix weight (mg)	D in the matrix (mg)	D release USP-intestinal solution		
			Slope (%/min)	Intercept	r^2 (n)[a]
$(AA–Me)_{50}$	200	82.8	2.23	−3.26	0.994
$(AA–Pr)_{50}$	200	75.8	0.89	0.66	0.997
$(AA–Me)_{50}$ + NaAA (1:3)	400	41.4	0.40	−1.41	0.998
$(AA–Pr)_{50}$ + NaAA (1:3)	400	37.9	0.28	11.74	0.986
Me + NaAA	400	41.4	–	–	–
Me.HCl + Na AA	400	45.5	–	–	–
Pr + NaAA	400	37.9	–	–	–
Pr.HCl + NaAA	400	41.1	–	–	–

[a] n, number of points. They cover a range of 0–80% of delivery.

such basis, Eqs. (1) and (2) are proposed to account for the dissociation of the complex $(AA–D)_x$ during delivery. There, R–COO^- and R–COOH represent carboxylic groups of AA while A^-M^+ a salt dissolved in the delivery medium.

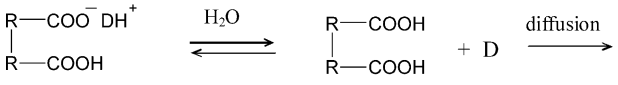

(1)

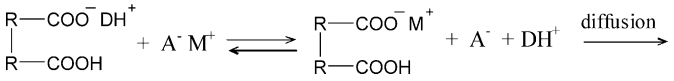

(2)

Such processes of dissociation that yield free D molecules would occur either in the hydrogel layer or furtherly in the dispersion of $(AA–D)_x$ delivered by erosion to the dissolution medium as depicted in Scheme 1.

During swelling of mixed matrices ($(AA–D)_x$ + NaAA), ionic exchange between $(AA–D)_x$ and NaAA should also occurs in same extent as depicted in Eq. (3):

$$(AA–At)_x + NaAA \rightarrow (Na–AA–At)_x. \quad (3)$$

Although the analytical methodology used to determine drug concentration in the delivery medium does not discriminate between $(AA–D)_x$ (or $(NaAA–D)_x$) and free D, the parallelism between matrix erosion and drug concentration suggests that the main process is the transference of the whole complex to the medium in which furtherly takes place the dissociation according to Eqs. (1) and (2).

To obtain complementary information on this point, aqueous dispersions of $(AA–At)_{100}$ were introduced in the upper compartment of a Franz cell, to measure the delivery of At to either water or NaCl solution placed in the receptor compartment. Both compartments were limited by a semipermeable membrane.

As Fig. 8 shows diffusion of At in water was very slow to reach a plateau after having delivered 8.95% of At, which indicates that equilibrium (1) remained shifted to the left. As 0.9% NaCl was placed in the receptor medium, diffusion rate increased as a consequence of the ionic exchange mechanism (Eq. (2)) generated by the diffusion of Na^+ and Cl^- to the upper compartment. This behavior contrasts with the observation that delivery from

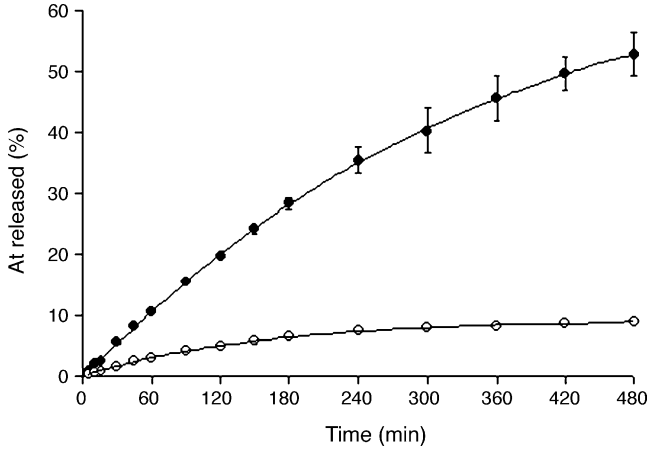

Fig. 8. At release from dispersions of $(AA–At)_{100}$ in distilled water (◯) and 0.9 NaCl solution (●).

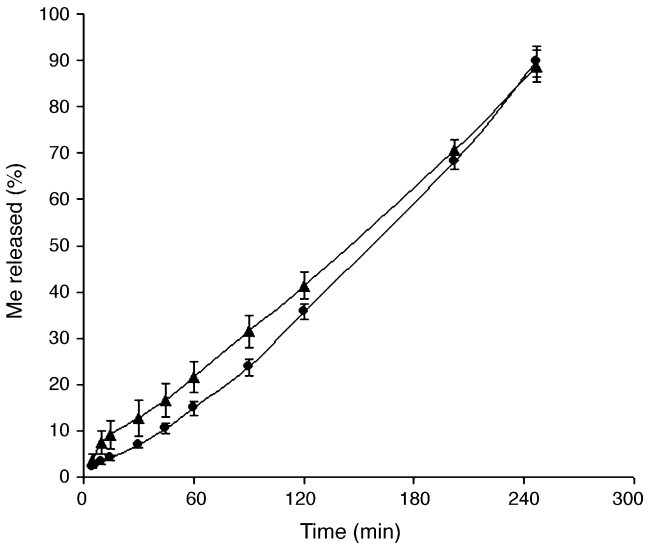

Fig. 9. Release profiles of Me from matrices in USP-intestinal solution: (●) Me + NaAA, (▲) MeHCl + NaAA.

SDPM in both water and saline buffer exhibited similar rates providing an additional evidence in favor of an erosion mechanism of the matrices.

3.6. In situ generation of the interaction between NaAA and D

It was considered of interest to know about the delivery performance of conventional matrices obtained by mixing NaAA with the free bases of At, Me and Pr such as it is reported in Table 3.

In order to generate an acid–base interaction during swelling, pH 6.8 saline buffer was selected as delivery medium. In addition, NaAA matrices of hydrochlorides of the two less soluble bases Me and Pr were also prepared. The matrix of the highest soluble drug At shown a delivery profile quite similar to that of

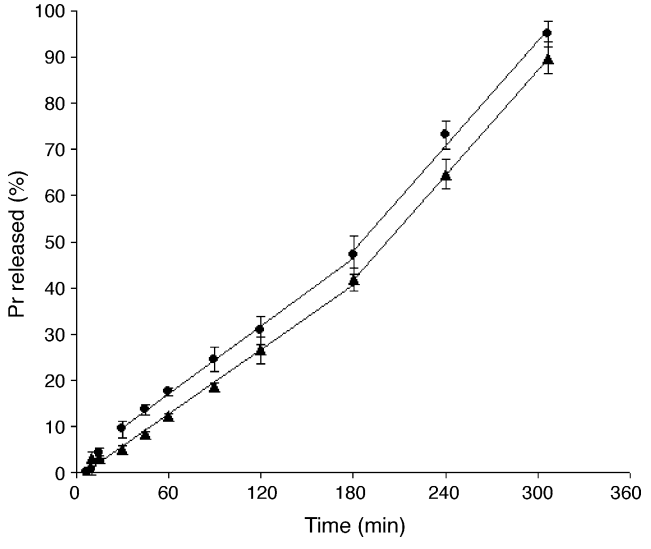

Fig. 10. Release profiles of Pr from matrices in USP-intestinal solution: (●) Pr + NaAA, (▲) PrHCl + NaAA.

$(AA–At)_{50}$ + NaAA (1:3), which suggests that dissolution rate of At was not the rate limiting step.

However, the matrix of Me exhibited a delivery profile (Fig. 9) that suggests that dissolution rate is involved in the control of delivery, while its hydrochloride matrix shown a similar profile to those of mixed SDPM.

On the other hand, as can be seen in Fig. 10, delivery profiles of Pr and PrHCl conventional matrices although exhibited the expected trend, they shown a departure from the linearity that was observed with $(AA–Pr)_{50}$ + Na AA (1:3) in the whole range of delivery (Table 3).

4. Conclusions

Present in vitro results shown that SDPM of $(AA–D)_x$ alone or in combination with NaAA exhibited a remarkable zero order of delivery in water and buffer of pH 6.8 and also in the two-step delivery experiments: 2 h in acid medium followed by a second step at pH 6.8. Experimental results indicate that the erosion of the hydrogel layer is the main delivery process. Therefore, delivery rate, being directly related to the proportion of D in the matrix, can be modulated either by varying the composition of $(AA–D)_x$ or by diluting it with NaAA.

Solid $(AA–D)_x$ complexes were easily prepared in the lab and would be obtained at higher scale with the current equipment of tablet technology.

On the other hand, as was early mentioned, carbomer–drug $(C–D)_x$ SDPM were previously evaluated in our lab (Jimenez-Kairuz et al., 2005). In such matrices, unlike the erosion control observed here with $(AA–D)_x$ SDPM, diffusion mechanism appeared to be the main delivery process.

Then, the different delivery mechanisms exhibited by AA and C based matrices should be primarily ascribed to differences in the physical properties of their respective hydrogel layers.

In fact, $(C–D)_x$ matrices generate a high viscosity hydrogel layer (667 mPa s, 0.25% $(C–At)_{50}$ dispersion) in which the entanglement among ramified polyelectrolyte chains prevents erosion, while $(AA–D)_x$ matrices generate a hydrogel layer of lower viscosity (82 mPa s, 5% $(AA–At)_{50}$ dispersion) in which linear $(AA–D)_x$ chains would be more easily eroded.

In conclusion, polyelectrolyte–drug complexes like $(C–D)_x$ and $(AA–D)_x$ exhibit interesting delivery properties and can find a place in the design of monolithic as well as multiparticulate delivery systems.

Acknowledgements

Financial support was received from CONICET, SECYT-UNC and FONCYT. The authors thank Ms. Marina Ardusso for her technical assistance and PhD María Eugenia Olivera for the paper revision. M.V.R.R. thanks CONICET for a research fellowship.

References

Bettini, R., Colombo, P., Massimo, G., Catellani, P.L., Vitali, T., 1994. Swelling and drug release in hydrogel matrices: polymer viscosity and matrix porosity effects. Eur. J. Pharm. Sci. 2, 213–219.

Bodmeier, R., Wang, J., 1993. Microencapsulation of drugs with aqueous colloidal polymer dispersions. J. Pharm. Sci. 82, 191–194.

Bonferoni, M.C., Rossi, S., Ferrari, F., Bettinetti, G.P., Caramella, C., 2000. Characterization of a diltiazem–lambda carrageenan complex. Int. J. Pharm. 200, 207–216.

Colombo, P., Bettini, R., Massimo, G., Catellani, P.L., Santi, P., Peppas, N.A., 1995. Drug diffusion front movement is important in drug release from swellable matrix tablets. J. Pharm. Sci. 84, 991–997.

Colombo, P., Bettini, R., Santi, P., De Ascentiis, A., Peppas, N.A., 1996. Analysis of the swelling and release mechanisms from drug delivery systems with emphasis on drug solubility and water transport. J. Controlled Release 39, 231–237.

Colombo, P., Bettini, R., Peppas, N.A., 1999. Observation of swelling and diffusion front position during swelling in hydroxypropylmethyl cellulose (HPMC) matrices containing a soluble drug. J. Controlled Release 61, 83–91.

Conley, R.T., 1979. Espectroscopia Infrarroja, 1 Spanish Ed. Alhambra SA, Madrid, Spain.

Ferrero, C., Muñoz-Ruiz, A., Jimenez-Castellanos, M.R., 2000. Fronts movements as a useful tool for hydrophilic matrix release mechanism elucidation. Int. J. Pharm. 202, 21–28.

Giunchedi, P., Gavini, E., Moretti, M.D.L., Pirisimo, G., 2000. Evaluation of alginate compressed matrices as prolonged drug delivery systems. AAPS PharmSciTech 1, article 19. http://www.aapspharmscitech.org (online journal).

Holte, Ø., Onsøyen, E., Myrvold, R., Karlsen, J., 2003. Sustained release of water-soluble drug from directly compressed alginate tablets. Eur. J. Pharm. Sci. 20, 403–407.

Huang, R.Y.M., Pal, R., Moon, G.Y., 1999. Characteristics of sodium alginate membranes for the pervaporacion dehydratation of ethanol–water and isopropanol–water mixtures. J. Membr. Sci. 160, 101–113.

Jimenez-Kairuz, A.F., 2004. Investigación y desarrollo de nuevos materiales con utilidad en tecnología farmacéutica para el diseño de sistemas terapéuticos. Ph.D. Thesis, Facultad de Ciencias Químicas, Universidad Nacional de Córdoba, Argentina.

Jimenez-Kairuz, A.F., Allemandi, D.A., Manzo, R.H., 2002. Mechanism of lidocaine release from carbomer–lidocaine hydrogels. J. Pharm. Sci. 91, 267–272.

Jimenez-Kairuz, A.F., Allemandi, D.A., Manzo, R.H., 2003. Equilibrium properties and mechanism of kinetic release of metoclopramide from carbomer hydrogels. Int. J. Pharm. 250, 129–136.

Jimenez-Kairuz, A.F., Llabot, J.M., Allemandi, D.A., Manzo, R.H., 2005. Swellable drug–polyelectrolyte matrices (SDPM). Characterization and delivery properties. Int. J. Pharm. 288, 87–99.

Kavanagh, N., Corrigan, O.I., 2004. Swelling and erosion properties of hydroxypropylmethylcellulose (Hypromellose) matrices—influence of agitation rate and dissolution medium composition. Int. J. Pharm. 279, 141–152.

Klaudianos, V.S., 1978. Alginat-retard-tabletten. Dtsch. Apoth. Ztg. 118, 683–684.

Llabot, J.M., Manzo, R.H., Allemandi, D.A., 2002. Double-layered mucoadhesive tablets containing nystatin. AAPS PharmSciTech 3, article 22. http://www.aapspharmscitech.org (online journal).

Munday, D.L., Cox, P.J., 2000. Compressed xantan and karaya gum matrices: hydratation, erosion and drug release mechanisms. Int. J. Pharm. 203, 179–192.

Nogami, H., Nagai, T., Fukuoka, E., Sonobe, T., 1969. Disintegration of the aspirin tablets containing potato starch and microcrystalline cellulose in various concentrations. Chem. Pharm. Bull. 17, 1450–1455.

Østberg, T., Lund, E.M., Graffner, C., 1994. Calcium alginate matrices for oral multiple unit administration. IV. Release characteristics in different media. Int. J. Pharm. 112, 241–248.

Pitré, D., Stradi, R., 1987. Metoclopramide hydrochloride. In: Florey, K. (Ed.), Analytical Profiles of Drug Substances, vol. 16. Academic Press, New York, pp. 1–25.

Rubio, M.R., Ghaly, E.S., 1994. In-vitro release of acetaminophen from sodium alginate controlled release pellets. Drug Dev. Ind. Pharm. 20, 1239–1251.

Sinha Roy, D., Rohera, B.D., 2002. Comparative evaluation of rate of hydration and matrix erosion of HEC and HPC and study of drug release from their matrices. Eur. J. Pharm. Sci. 16, 193–199.

Soares, J.P., Santos, J.E., Chierice, G.O., Cavalheiro, E.T.G., 2004. Thermal behavior of alginic acid and its sodium salt. Ecl. Quím. São Paulo 29, 53–56.

The Merck Index, 1996. 12th ed. Merck & Co., Inc., Whitehouse Station, NJ, USA, p. MISC-60.

Tu, J., Bolla, S., Barr, J., Miedema, J., Li, X., Jasti, B., 2005. Alginate microparticles prepared by spray-coagulation method: preparation, drug loading and release characterization. Int. J. Pharm. 303, 171–181.

Ughini, F., Andreazza, I.F., Ganter, J.L.M.S., Bresolin, T.M.B., 2004. Evaluation of xantan and highly substituted galactomannan from M Scabrella as a sustained release matrix. Int. J. Pharm. 271, 197–205.

Vilches, A.P., Jimenez-Kairuz, A.F., Alovero, F., Olivera, M.E., Allemandi, D.A., Manzo, R.H., 2002. Release kinetics and up-take studies of model fluoroquinolones from carbomer hydrogels. Int. J. Pharm. 246, 17–24.

Wade, A., Weller, P.J., 1994. Handbook of pharmaceutical excipients. In: American Pharmaceutical Association, 2nd ed. The Pharmaceutical Press, Washington, DC, USA, pp. 10–11, 428–429.

Zuleger, S., Lippold, B.C., 2001. Polymer particle erosion controlling drug release I. Factors influencing drug release and characterization of the release mechanism. Int. J. Pharm 217, 139–152.